Geospatial Nexus of Land Use Land Cover dynamics and Rapid Population Growth with Emphasis on Trend Prediction of Built-Up Areas in District Hangu, Pakistan

Farishta Khan, Atta-Ur Rahman, Uzma Manglore, Shazia Dilbar
Department of Geography and Geomatics, University of Peshawar, Pakistan
*Correspondence: farshta89654@gmail.com

Citation | Khan. F, Rahman. A. U, Manglore. U, Dilbar. S, "Geospatial Nexus of Land Use Land Cover dynamics and Rapid Population Growth with Emphasis on Trend Prediction of Built-Up Areas in District Hangu, Pakistan", IJIST, Vol. 07 Special Issue. pp 157-173, August 2025
Received| July 21, 2025 **Revised|** August 03, 2025 **Accepted|** August 08, 2025 **Published|** August 10, 2025.

This study aims to analyze the land use land cover (LULC) and predict the patterns in the built-up areas of District Hangu and examine how population growth affects land use and land cover. Rapid population increase remains a continuous threat to the district's land resources. Projections show that the population will grow from 518,811 in 2017 to 833,964 by 2051. Along with this growth, there is an ongoing expansion of underground utilities and infrastructure, driven by demographic pressures and urban development. The Logistic Regression (LR) model was used to forecast an expansion in the district's built-up area. Through this model, potential zones for future development are identified, and anticipated changes in planned Land Use/Land Cover (LU/LC) are evaluated. All variables were transformed into raster format and standardized to a 0–1 range using a raster calculator, ensuring uniformity in statistical comparisons. Factor standardization played a central role in the multivariate analysis, where the Variance Inflation Factor (VIF) method in SPSS was applied to resolve multicollinearity issues. Predictors with VIF values exceeding 10 were substituted with alternatives falling below this limit. Land use and land cover data were obtained from Landsat images for the years 1991, 2001, 2011, and 2021, each at a 30-meter resolution. Results indicate that the proportion of built-up areas increased from 8% in 1991 to 11% in 2021, while vegetation cover decreased from 43% to 45%. During the same period, barren land reduced from 47% to 40%, and water bodies expanded from 3% to 4%. Future projections of built-up areas identify the most suitable zones for urban growth. The LR model integrates multiple variables such as railways, primary roads, tracks, commercial zones, educational and health facilities, and economic hubs using tools including SPSS, IDRISI, and ArcMap. IDRISI Selva is applied for future land use modeling, estimating that built-up areas will cover 161.22 km² by 2050. The prediction results indicate that population growth will continue to be a significant driver of built-up expansion in Hangu District.

Keywords: Land Use Land Cover, Population Growth, Built-up Areas Logistic Regression Model., IRISI Salva, SPSS

Introduction:

Population growth has been unpredictable throughout history. The records show that the death rate was consistently lower than the birth rate, and population growth was rarely greater than zero [1]. In the past, as people started farming and keeping animals, population growth increased slowly [2]. The world population grew from 800 million in 1750 to 7.6 billion in 2016 [3]. Every year, between 75 and 80 million new individuals are added to the world population [4]. By 2025, estimates indicate that there will be 8 billion people on earth, and by 2050, there will be 9 billion people if the current rate of population growth continues [5]. Since there is human intervention in the entire ecosystem, there is a persistent shift in Land Use Land Cover (LULC) as an outcome of population growth. This has an important influence on the local, regional, and global environments [6].

When analyzing how humans interact with their environment, land use and land cover are important variables [7]. Land Use and Land Cover (LULC) changes are highly dynamic in the context of global environmental shifts [8]. Alterations in land use and cover have contributed to increased flooding during natural disasters, biodiversity and vegetation loss, and the acceleration of global warming [9]. Geographic variations in LULC significantly influence environmental conditions [10]. Land use change is recognized as a primary driver of environmental transformation and one of the most critical sustainability challenges facing the world today. Understanding the modifications within the built environment and the complex interactions between human activities and natural systems is therefore essential [11]. Human actions are the main cause of LULC variations, which impact the Earth's surface by altering energy balance, energy flows, and atmospheric mixing processes, ultimately contributing to global climate change [12].

The influence of rapid population growth on land cover and the utilization of land has led to substantial changes and diversification in LULC [13][14]. Pollution, the loss of natural habitats, and a decline in environmental quality are the main consequences of the LU/LC change [15]. Variations in rainfall intensity and frequency, flash floods, global warming, and climate change are due to population growth [16] The earliest human activity was agriculture [15]. One of the biggest and most serious challenges facing people is the reduction of agricultural land availability, which leads to a shortage of food due to built-up land increasing with time, which may cause desertification, waterlogging, and salinization [17]. Agricultural land is the primary source of food and raw materials worldwide [18].

Due to environmental, socioeconomic, and human activity, an area's land use and land cover can change over time. Variations in Land Use and Land Cover (LU/LC) are affected by different factors, including population growth, economic development, and physical characteristics, as well as climate, topography, slope condition, and soil type [16][13]. Research on land use and forests shows that migration is the primary factor related to population that causes LU/LC change. Population growth, population density, and dispersion over longer periods have been found to have a significant effect on land use, forest quality, and forest area [13][19].

The population of Pakistan is growing at 2.1% per year. To meet the requirements of an expanding population for housing, agriculture, commercial expansion, and the manufacturing of other necessities for daily life, more land is required. According to [20], the rapid growth rate has resulted in deforestation, urban sprawl, and agricultural land degradation. The LU/LC change pattern in Pakistan is not significantly different from global patterns.

Method and Material:

The Study Area:

Hangu District, situated in the Kohat Division of Khyber Pakhtunkhwa Province, Pakistan, spans an area of about 1,380 square kilometres (km^2). It shares its western boundary with Kurram District, its northern boundary with Orakzai District, and is bordered on the east

by Hangu, Kohat, and Karak districts. North Waziristan lies to its south. Geographically, the district extends between latitudes 33°15' and 33°35' N and longitudes 70°29' and 71°14' E (Figure 1).

The region lies at elevations ranging from 900 to 1,495 meters above sea level, with Thal being the highest point at 1,495 meters. Major watercourses include Nasar Toi in the east and Shkalai Nulah in the west. Hangu has a humid climate, experiencing hot summers and cold winters, with rainfall occurring throughout the year. The district receives an average annual rainfall of about 536 mm, with a mean yearly temperature of 20.7 °C. June records the highest average temperature at 31.1 °C, while January is the coldest month, averaging 9.1 °C. Topographically, a valley runs from southwest to northeast through the district's center, surrounded by hills and mountains. Figure 1 shows the location map.

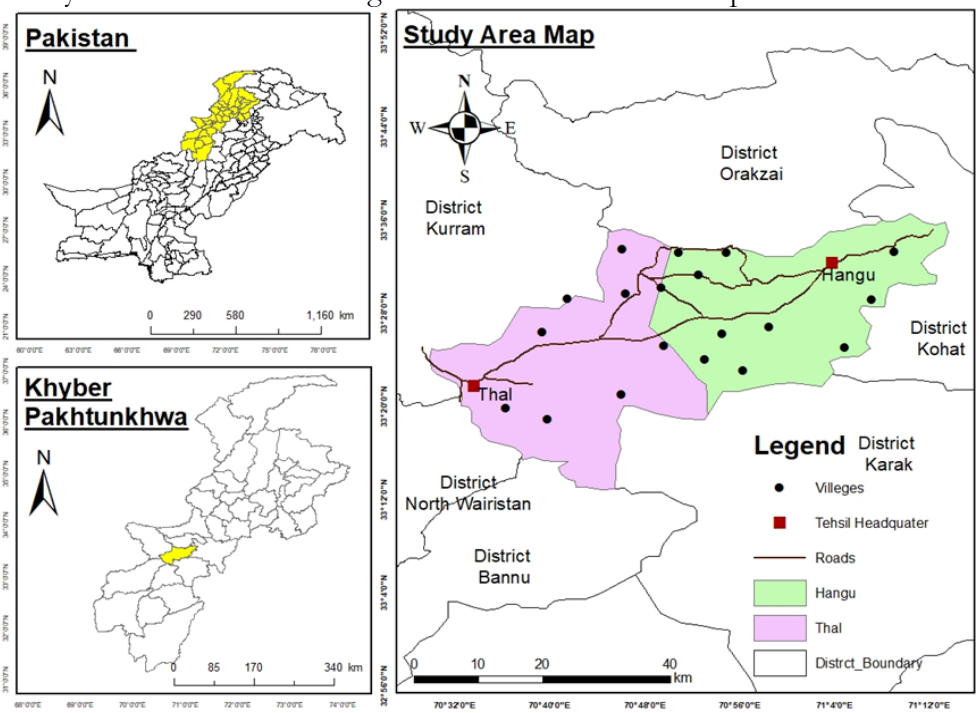

Figure 1. District Hangu, Study Area Location

Data Collection:

The data were collected from a secondary source. Secondary data were gathered from various departments, such as the KP Board of Revenue (BoR) department and the Pakistan Bureau of Statistics (PBS). In addition, data were collected from satellite images from 1991, 2001, 2011, and 2021, which were downloaded from the USGS Website (www.usgs.com). One image covers the whole study area. Spatial and temporal changes in LULC in Hangu District from 1991 to 2021 were obtained from satellite images. Data are divided into three groups according to their types: remote sensing data, statistical data, and vector datasets. Demographic information was obtained from Pakistan census data for 1961, 1972, 1981, 1998, and 2017.

Secondary and Remote Sensing Data:

Satellite imagery was obtained from the USGS with 30-meter resolution and collected for different years (1991, 2001, 2011, and 2021). Population data were collected from the district census report for 1998-2017. Tehsil-wise data for 2021 are sourced from the KP Board of Revenue (BOR), while other statistical data are from the Pakistan Bureau of Statistics (PBS), Peshawar.

Land Use and Population Census Data:

A census is a general procedure for collecting and recording demographic information about all people in a specific area at a specific time. The government conducts censuses as the

most reliable source of population data. Land use data show variations in land use over time. With population growth, the landscape of agricultural land changes in the study area.

Satellite Images:

ArcGIS ArcMap 10.5 version was used to assemble and analyze satellite images. The image has been imported into a GIS environment. Images with a resolution of 30 meters are freely available on the website. Thus, for research and study, images of different time intervals were obtained from their website. We collected images for different years i.e., 1991, 2001, 2011, and 2021. The properties of satellite images are shown in Table 1.

Table 1. District Hangu, Features of the Satellite Images

Dataset	Year	Resolution	Sources	Projection Purpose
Landsat	1991	30 meters	USGS UTM zone 42N	For preparing the LU/LC map
Landsat	2001	30 meters	USGS UTM zone 42N	For preparing the LU/LC map
Landsat	2011	30 meters	USGS UTM zone 42N	For preparing the LU/LC map
Landsat	2021	30 meters	USGS UTM zone 42N	For preparing the LU/LC map

Methods and Process of Data Analysis:

The study follows a logical framework and a structured approach for analyzing and effectively presenting the collected data. While the primary objective was to identify built-up development using population data for Hangu from 1991 to 2021, the unavailability of census data beyond 2017 required estimating the 2021 population through statistical methods. These estimates were then used to interpret patterns of urban expansion in the district. To capture observable trends in urban growth, the study period was extended to 2021.

Satellite imagery from 1991 to 2021 was analyzed in distinct temporal intervals. All images were geometrically aligned to a consistent projection and analyzed through supervised classification. This process enabled the extraction of reliable information on land use changes. Each image covered the entire study area. The overall research methodology is illustrated in the flowchart presented in Figure 2.

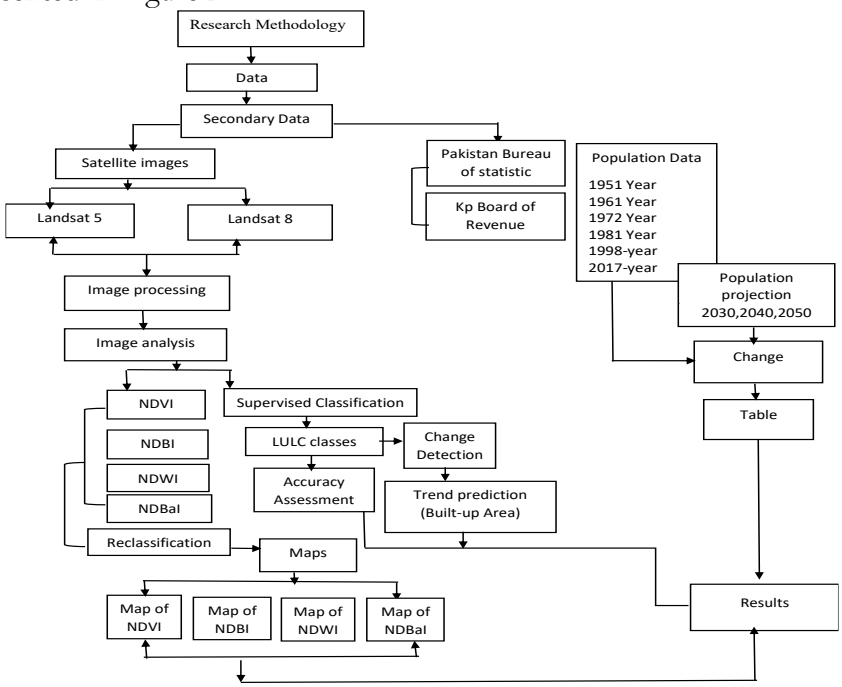

Figure 2. District Hangu, Research Methodology Flow Chart

Results, Analysis and Discussion:

Land Use Land Cover Classes 1991-2021:

Between 1991 and 2021, District Hangu experienced notable shifts in both land cover and land use. The built-up area expanded from 111.88 km² (8%) in 1991 to 149.24 km² (11%)

in 2021, whereas vegetation cover grew from 577.58 km² (43%) to 622.32 km² (45%) over the same period. In 1991, 648.49 km² (47%) of the land was covered by barren land; by now, that percentage had dropped to 560.92 km² (40%). Table 2 and Figures 3 and 4 show the final results.

Table 2. District Hangu, Land Use Land Cover Classes 1991-2021

LU/LC Classes	Area in (km²) 1991	Area 1991 (%)	Area in (km²) 2021	Area 2021 (%)	Change (%)
Vegetation	577.58	43	622.32	45	2
Built-up	111.88	8	149.42	11	3
Water Bodies	42.60	3	49.42	4	1
Barren Land	648.49	47	560.92	40	7
Total Land	**1380**	**100**	**1380**	**100**	**16**

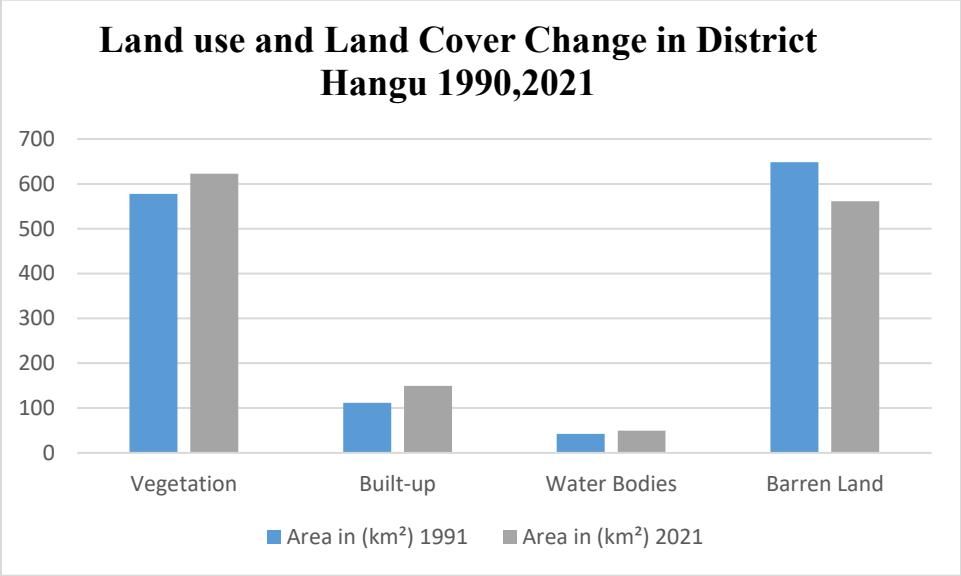

Figure 3. District Hangu, Land Use Land Cover Classes

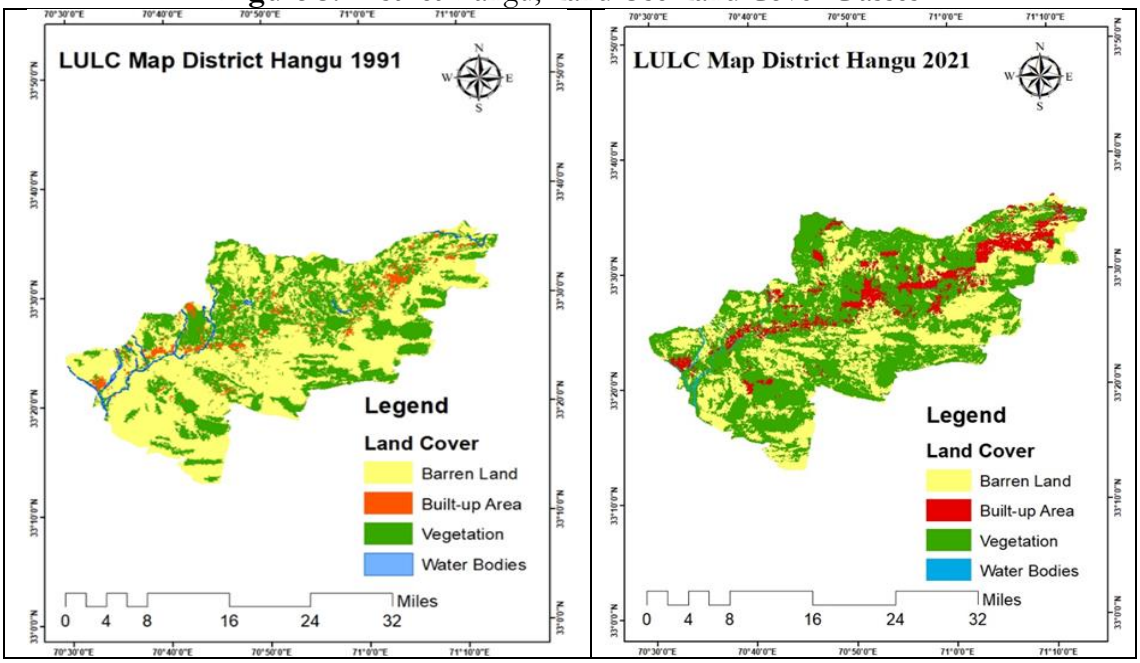

Figure 4. District Hangu, Land Use Land Cover Classes

Land Use Land Cover Classification (1991-2021):

Land use and land cover maps of District Hangu have multiple classes that show various values. Built-up extent was 111.88 km² in 1991 and 124.44 km² in 2001, and it increased with

time, and in 2011 the value showed a variation of 132.25 km². District Hangu had a slight increase in this area, and similar land use values showed that the built-up area expanded to 149.24 km² in 2021. The vegetation cover varies with time as well. In 1991, it covered 577.58 km², but by 2001, it had grown to 638 km², and by 2021, it had dropped to 630.23 km². Figure 5,6 and Table 3 show the results.

Table 3. District Hangu, Land Use Land Cover Classes 1991-2021

LU/LC Classes	1991	2001	2011	2021
Vegetation	**577.58**	**638.00**	**630.23**	**622.32**
Built-up	**111.88**	**124.44**	**132.25**	**149.24**
Water Bodies	**42.60**	**37.05**	**46.54**	**49.42**
Barren Land	**648.49**	**581.11**	**571.11**	**560.92**

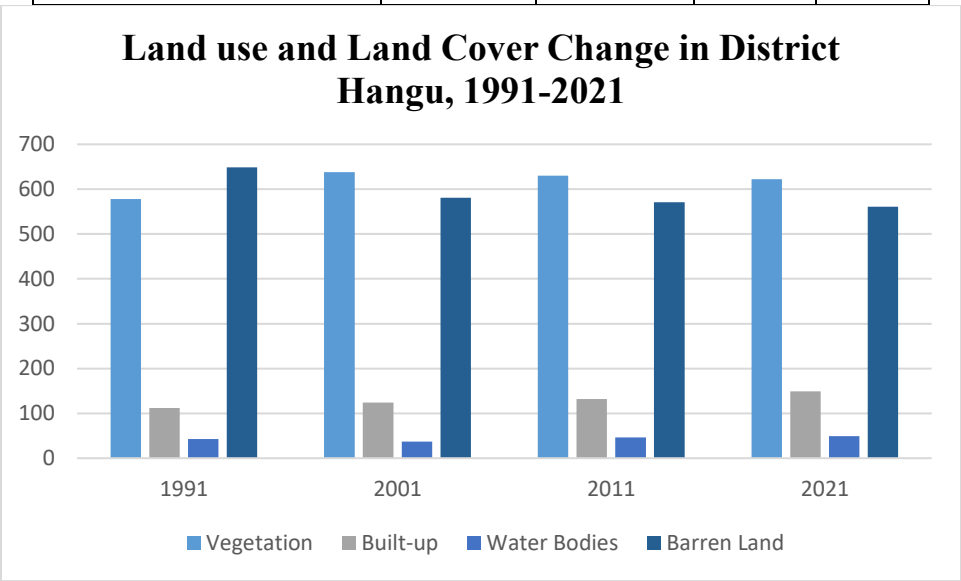

Figure 5. District Hangu, Land Use Land Cover Classes 1991-2021

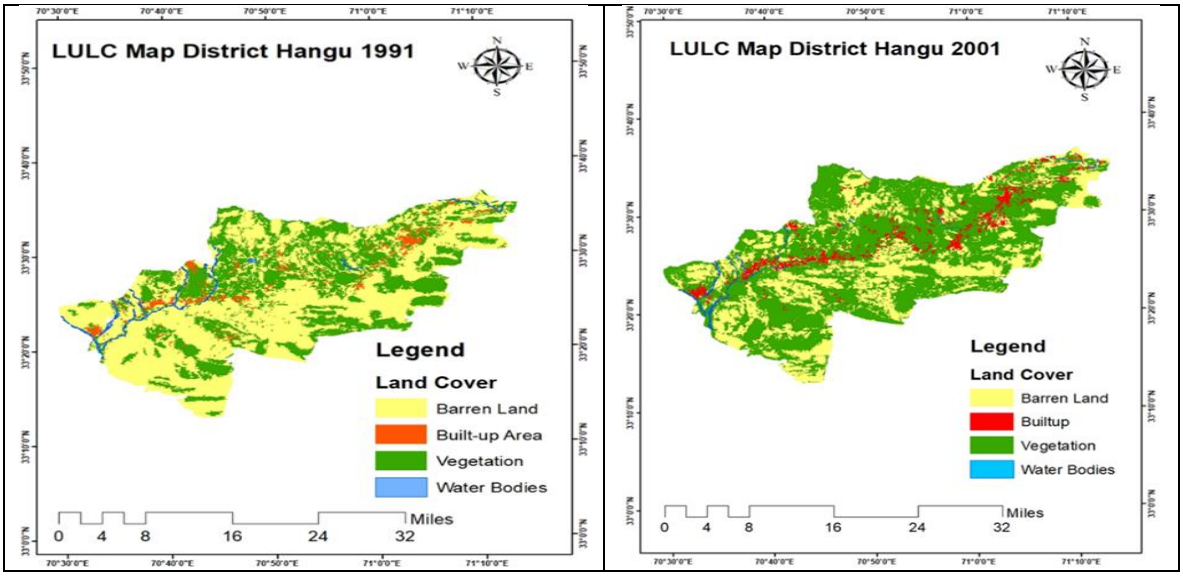

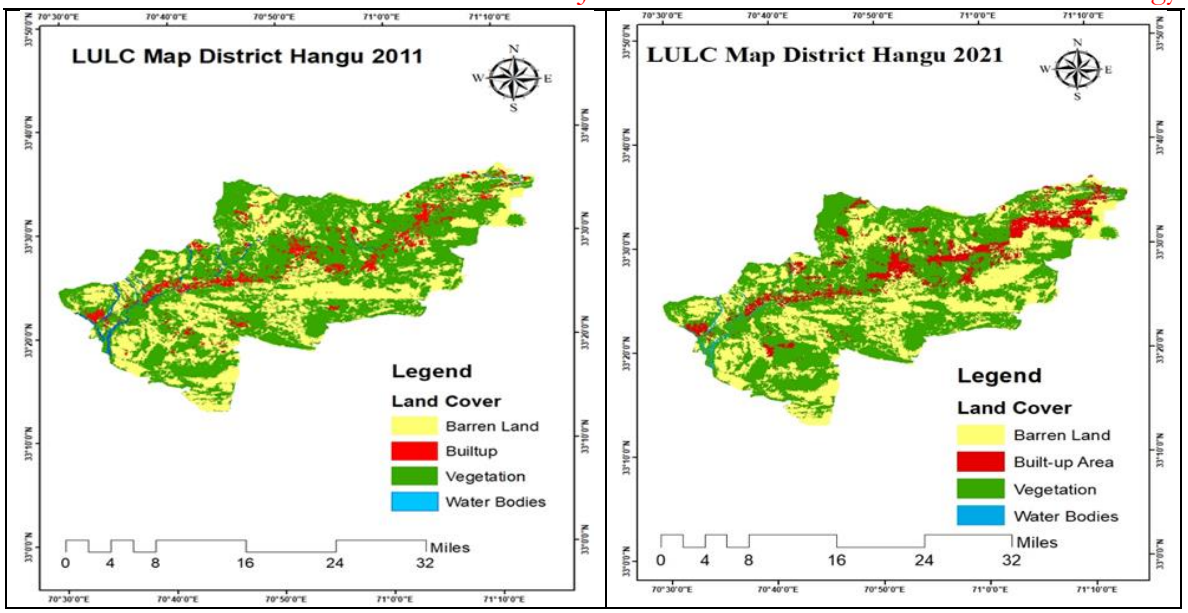

Figure 6. District Hangu, Land Use Land Cover Classes (1991-2021)

Accuracy Assessment:

The accuracy of the Land Use and Land Cover (LU/LC) maps was evaluated by comparing the classified land use categories with reference data obtained from satellite imagery. A pixel-by-pixel accuracy assessment was performed using 240 randomly distributed points on the LU/LC maps for the years 1991, 2001, 2011, and 2021. These points were cross-verified against spatial maps and satellite images to confirm classification results, with each point representing a specific land use category.

A confusion matrix was generated from the intersected data to identify misclassified pixels. The matrix provided values for producer accuracy (based on classified points), user accuracy (based on reference points), overall accuracy, and the kappa coefficient. An overall accuracy of at least 90.8% was considered acceptable for LU/LC classification. The results showed overall accuracies of 90.8% (1991), 93.0% (2001), 93.0% (2011), and 94.0% (2021). The corresponding kappa coefficients were 1.10, 1.12, 1.30, and 0.90, respectively.

Water bodies and wetlands exhibited higher classification accuracy due to their distinct spectral signatures. In contrast, barren land was occasionally misclassified as built-up areas because of similar pixel reflectance values. Misclassification was more likely in areas with a high concentration of mixed pixels representing multiple land use categories. The overall classification accuracies for each year are summarized in Table 4.

Table 4. District Hangu, Overall Accuracy

Year		**1991**	**2001**	**2010**	**2021**
Type of Accuracy	**LU/LC**	**%**	**%**	**%**	**%**
Producer Accuracy %	Water	81.6	5.0	85.0	90.6
	Built-up	93.3	93.3	93.3	92.6
	Vegetation	93.3	95.0	95.0	92.0
	Barren Land	95	91.6	91.6	96.3
User Accuracy %	Water	96.0	99.0	92.7	89.9
	Built-up	94.9	98.0	96.5	93.2
	Vegetation	93.4	78.7	96.6	98.0
	Barren Land	81.1	99.0	80.8	77.9
Overall Accuracy %		90.8	93	93	93
Kappa Coefficient		1.10	1.12	1.3	0.9

Trend Prediction in Built-Up Area and Population Projection:

The forecasting of urban growth and the application of forecasting methods for expected urban growth. Early in the 20th century, the model known as logistic regression was applied in the biological sciences. Later, it was modified for use in a number of social science fields. When the target, is definite, prediction model is used.

Future population size estimates are dependent on factors such as migration, birth rate, mortality rate, and population size [21]. Constant foundation in a "conditional" future. For upcoming population forecasts, population projections should be sufficient. Three factors affect a nation's potential population: mortality, migratory patterns, and fertility. The starting population for a population projection is usually the population at a certain point in time, broken down by age and gender. The population projections are based on these projections of future migration, death, and fertility [22]. This will be the process of estimating the population for the years 2030, 2040, and 2050.

Characteristics of Population:

The main drivers of population growth include a high birth rate, low mortality rate, and significant natural increase. Additionally, the labor force constitutes a smaller share of the total population, resulting in a high dependency ratio. Rapid urbanization, often accompanied by inadequate family planning, also fuels this growth. Migration is another key factor that accelerates population expansion. Common demographic characteristics include competition, age distribution, gender composition, and societal structure.

By using the Statistic Mean Formula: $Pn = P_{\circ} + nx$ Here P_n is represents the Last population x Represented inter-censual population change $P_{\circ}$ is for the next population N Shows the number of decades [23]

Population Projection:

Population projections estimate future population size along with its age and sex distribution. These forecasts are based on historical trends and consider three key variables: migration, mortality, and fertility. Various assumptions regarding the future course of each factor are applied to generate multiple projection scenarios.

Population Growth in District Hangu 1961-2021:

Data on increase in population was obtained from the District Census Report (DCR) From 1961 to 2017. The population grew quickly from 108,647 in 1961 to 518,811 in 2017. This rapid population increase had a variety of repercussions on the land, including a rapid loss of vegetation cover that harmed land use and land cover. Additionally, the population projection for the future is made using a statistical technique. The population projections for the future show that it will be 647,824 in 2031, rise to 740,894 in 2041 as a result of the population's strong growth, and reach 833,964 in 2051 (Table 5; Figure 7).

Table 5. District Hangu, Population Growth 1961–2021

Year	Area (km²)	Total Population
1961	**1,380**	**108,647**
1972	**1,380**	**153,603**
1981	**1,380**	**182,474**
1991	**1,380**	**275,544**
2001	**1,380**	**368,614**
2011	**1,380**	**461,684**
2021	**1,380**	**554,754**

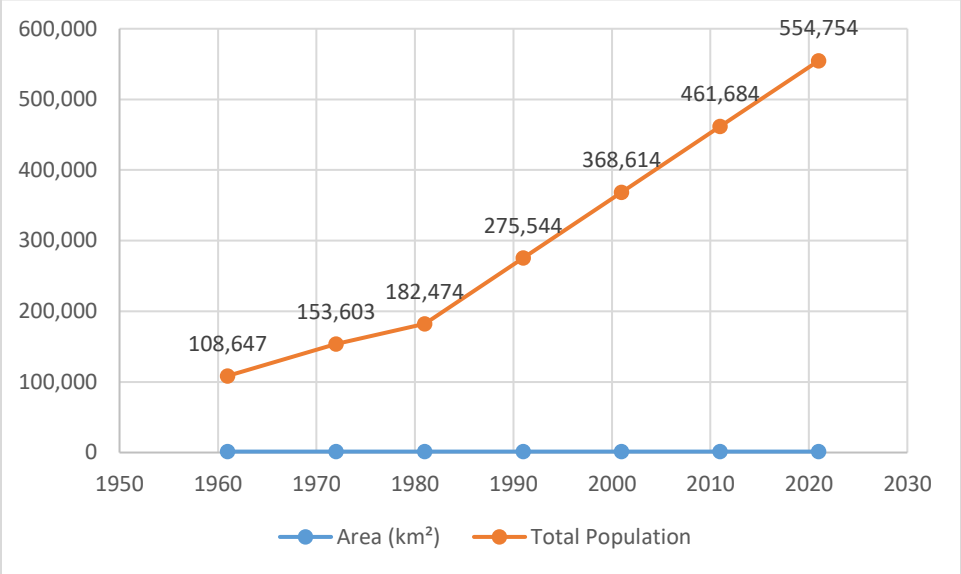

Figure 7. District Hangu, Population growth 1961-2021

Population Growth and Population Prediction in District Hangu 1991-2051:

The District Census Report (DCR) provides data on population growth from 1961 to 2017. The population was 108,647 in 1961 and 518,811 in 2017. The rapid population expansion had a variety of repercussions on the land, including a quick drop in vegetation cover, which harmed land use and land cover. Determining the population for the years 2031, 2041, and 2051 using the statistical algorithm technique of projection. Furthermore, population estimates for the future indicate that it will be 647,824 in 2031, rise to 740,894 in 2041 as a result of the population's strong growth, and reach 833,964 in 2051. Figure 8 and Table 6 display the population increase results from 1961 to 2051.

Table 6. District Hangu, Population growth 1961-2050

Year	Area (km²)	Total Population
1961	**1,380**	**108,647**
1972	**1,380**	**153,603**
1981	**1,380**	**182,474**
1991	**1,380**	**275,544**
2001	**1,380**	**368,614**
2011	**1,380**	**461,684**
2021	**1,380**	**554,754**
2031	**1,380**	**647,824**
2041	**1,380**	**740,894**
2051	**1,380**	**833,964**

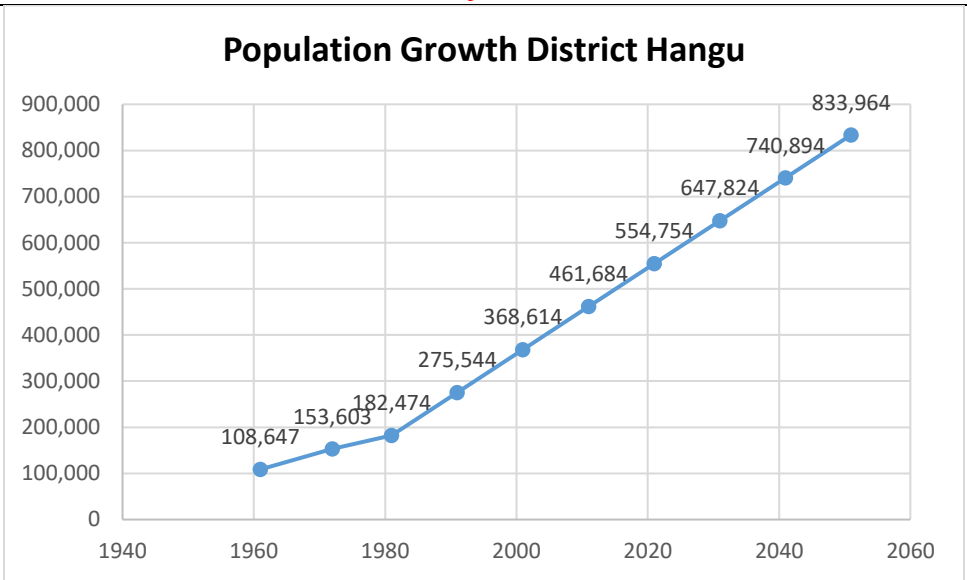

Figure 8. District Hangu, Population Growth

Growth Model for District Hangu:

Regression analysis is a statistical approach used to determine the best model for examining relationships between multiple independent variables and one or more dependent variables. It uses observed values of predictor variables to estimate the probability of occurrence or non-occurrence of an event. Independent variables may be continuous, categorical, or binary, while dependent variables can also be categorical or binary. A notable advantage of regression analysis is that it does not require the assumption of normality. For example, regression can be applied to analyze functional relationships between spring locations and factors influencing their formation.

The general linear regression equation is:

$$Y=a+b_1 X_1+b_2X_2+\cdots+bmXmY$$

where Y is the linear combination of explanatory variables X_1, X_2…, Xm are the coefficients to be estimated. In binary logistic regression, the dependent variable z takes the value 1 when the event is present and 0 when absent. The probability P that z=1 is modeled as the natural logarithm of the odds ratio.

Application of Regression Model for Trend Prediction:

A regression model explains the statistical relationship between one or more independent variables (Xi) and a dependent variable (Yi), including an error term (ei) to represent the variation not explained by the model. Yi=f(Xi, β) +ei Yi = f(Xi, \beta)

Here, β represents the unknown parameters of the model. Regression analysis helps evaluate how changes in independent variables are associated with changes in the dependent variable, making it suitable for trend prediction in urban growth modeling.

Acquisition of Data:

The study utilized secondary data from multiple sources, grouped into three categories: vector datasets, statistical data, and remotely sensed imagery. Demographic data were obtained from the Pakistan Bureau of Statistics (PBS), while land value information for 2021 categorized by Union Council was sourced from the Khyber Pakhtunkhwa Board of Revenue. Vector datasets from PBS included administrative boundaries, road networks, land values, and locations of public services, all projected in the Modified UTM coordinate system (Everest datum).

Remotely sensed data were processed alongside vector and statistical data to provide inputs for the regression model. The sources of data used in the regression analysis are detailed in Table 7.

Table 7. District Hangu, Data Source, Description, and Purposes

Data source	year	Source	Description	Purpose
Administrative Boundaries	2021	Pakistan Beaure of Statistic	District Hangu UC-wise boundaries	Delineating study area extends
Road Network	1991-2021	Pakistan Beaure of Statistic	Roads, Railway etc	Roads were used for proximity analysis
Public services	1991-2021	Pakistan Beaure of Statistic	Schools, collages hospitals, industries etc	Public services data use for proximity
Lans Use	1991-2021	USGS	Land use map of vegetation cover, built-up, Barren land, water bodies	Land use map for preparing landcover

Prediction-Related Factors:

The factors that make up the data used to create the regression model, such as proximity to major routes, post offices, railways, hospitals, and other enterprises, are grouped into multiple groups. Along with the data input and factor maps in Table 8 and 9, the factor maps are shown in Figure 9.

Table 8. Factors Map were Included in the Logistic Regression Model

Catagory	Factors
Proximity causes	Distance from Roads Distance from post office Distance from railway line Distance from Health centers Distance from education institution Distance from economic centers
Economic factors	Land Value

Table 9. Logistic Regression Model Input Data

Catagory	Factors	Nature of Variables
Nearness and factor of accessibility	Distance to:	Continuous
	Roads Railway Health centers Education institution Post office Economic centers	
Economic factors	Land Value	Continuous

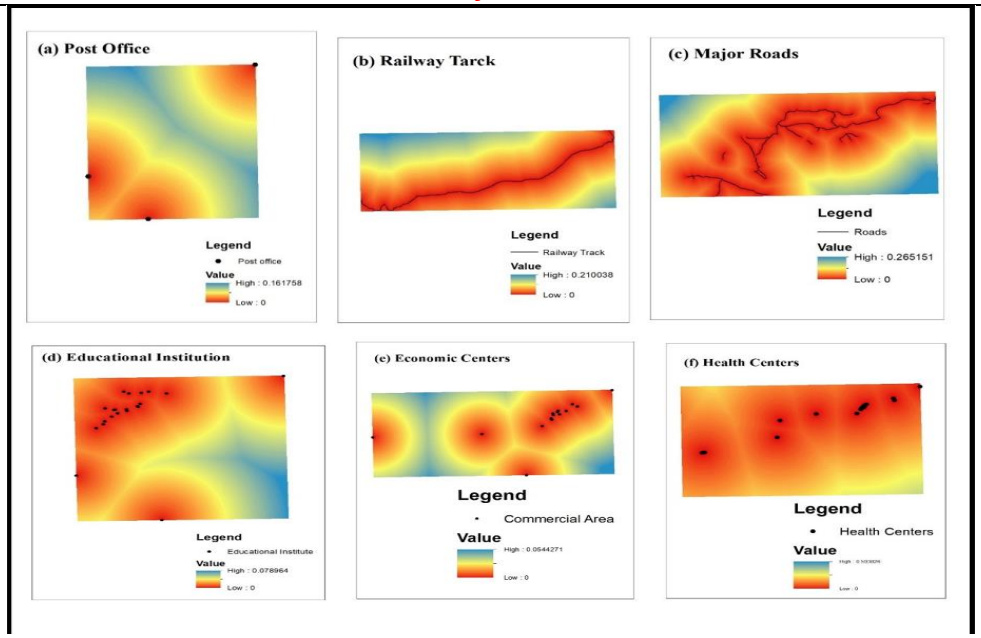

Figure 9. District Hangu, Factors Map 2021

Data Normalization for the Logistic Regression Model:

Each component of the input data was created using raster files. The standardization of the data made it fall between 0 and 1. Using a raster calculator, the input raster was normalized to produce a comparable data range in the GIS context. This approach, which we named logistic regression, is essential for multivariate statistical analysis. When comparing variables that fall within a similar range, it is essential to use the same unit of measurement for all. This can be ensured through the process of normalization.

Fishnet Tool Test for the Model:

The data from the attribute table were transformed into a CSV file using the Fishnet tool, and this file was subsequently imported into SPSS to examine the possibility of multicollinearity among the independent variables.

Multi-Collinearity Analysis:

A sign of a potential relationship between the independent variables is called collinearity. A multi-collinearity checks on the data should be the first step in any regression study. Every factor map's level of multicollinearity was examined independently. The effectiveness of the estimate's variable may decrease when the independent variable's collinearity rises. Therefore, before doing any regression analysis, it is imperative to verify that the independent variables are multicollinear. Multicollinearity was computed using the Variance Inflation Factor (VIF) in this analysis. From a statistical perspective, the Variance Inflation Factor (VIFi) is calculated as $VIFi = 1/1-R^2$where R^2 represents the coefficient of determination obtained by regressing the ith predictor against all other predictors included in the model.

All predictors except for the ith predictor are contained in the model coefficient of determination, or R2, in this instance. Therefore, the Logistic Regression (LR) model only contained variables with a VIF of 10. Eliminate from the study any independent variable with a VIF value of 10 [24]. It would be necessary toward ascertain the VIF for the surviving variables following the removal of the one that had a VIF larger than 10. Continue doing this until the VIF of each variable is less than 10.

The Logistic Regression Model's Fit Quality:

The appropriateness and good fit of logistic regression were assessed using the chi-square test. The accuracy to which the discovered values match the predicted values is

determined using numerical tests. Examined is the unimportant hypothesis, which holds that independent variables have no effect on the model's result [25].

Chi-square (x_2) = ∑ (observed value – predicted value)2 / predicted value: is the formula for the chi-square test.

Regression Model Evaluation and Percentage Correct Prediction (PCP):

The percentage of accurate predictions was used to test and validate the model analysis. One helpful indicator for evaluating the Logistic Regression model's goodness of fit is the percentage of Correct Predictions (PCP) [23]. The percentage of observations that are correctly forecast is a clear definition of it.

Formula for Percentage Correct Prediction (PCP): PCP= Number of Correct predictions / Total number of predictions × 100. Here PCP is an effective measure of model goodness of fit [26]. A useful indicator of model goodness of fit is PCP.

Prediction and Urban Growth:

Using the IDRISI Selva Edition, an urban growth probability map for 2050 was generated. The projections indicate that the built-up area in Hangu District will expand further, driven by continuous population growth. This expansion is expected to occur predominantly near commercial hubs and educational institutions, in response to increasing demands for schools, universities, markets, and healthcare facilities.

Logistic Regression Model for Year 2021:

Regression models are used to express a variable dependence on another variable, referred to as the independent variable. Based on the values of the independent variable that are found, regression provides an equation to predict the dependent variable's normal value. The logistic model parameter is shown in Table 10 below.

Table 10. Characteristics and Factors of the Logistic Regression Model 2021 District Hangu

		Unstandardized Coefficients		Standardized Coefficients	Sig.	Collinearity Statistics	VIF
		B	Std. Error	Beta		Tolerance	
1	Distance to Railway	-280.949	0.000	-478	0.123	0.433	2.11
	Distance to Major roads	-2832.090	0.000	-0.720	0.108	0.923	1.084
	Distance to post office	-9198.171	0.000	0.410	0.133	0.286	3.501
	Distance to Educational Institute	-789.403	0.000	-403	0.661	0.286	3.614
	Distance to Health Centers	-1677.22	0.000	-233	0.226	0.277	2.132

Application of Regression Model on Built-up Area:

The model summary is shown in Table 11 below. The Logistic Regression model estimates that the R-value is 0.973, with a standard error of 18.563 and a confidence level of 0.946.

Table 11. Shows the model summary.

MODEL SUMMARY			
R	**R Square**	**Adjusted R**	**Std. Error of the Estimate**
0.973	0.946	0.919	18.563
The independent variable is population			

Variance Analysis (ANOVA) of the Regression Model:

Some arithmetical analysis tool called analysis of variance (ANOVA) and the detected collective unpredictable data set is separated into two categories: random components and systematic variables. In the given data set, the systematic component has a statistical impact, while the random influences do not. Researchers utilize the ANOVA exam to find the impact of independent factors on the dependent variable. A two-way study of variance (ANOVA) uses 2 independent variable quantity, whereas a one-way ANOVA uses just one. This statistical test looks at the differences between more than two groups. The statistical ANOVA is shown in Table 12.

Formula for ANOVA is: F = MSB/MSE, the term "mean sum of squares" (MSE) owing to error, Mean Sum of Squares (MSB) due to treatment, and F for the ANOVA coefficient.

Table 12. Showing the ANOVA Statistical

	Sum of Squares	**df**	**Mean Square**	**F**	**Sig.**
Regression	12048.650	1	12048.650	32.964	0.027
Residential	689.194	2	344.597	-	-
Total	12737.844	3	-	-	-

Coefficient of the Regression Model:

Both standardized and unstandardized coefficients are typically generated by statistical software as default outputs. These coefficients indicate the predictable (linear) change in the outcome variable for each unit change in a given predictor. In this case, the coefficient value is $\beta - 0.5$, with the results summarized in Table 13.

Table 13. Showing the Coefficients of the Independent Variable

	Unstandardized Coefficients		**Standardized Coefficient**	**t**	**Sig.**
Population	**B**	**Std. Error**	**Beta**		
	0.01	0.000	0.73	5.913	
Constant	50.236	30.176	-	1.316	0.39

Growth of Regression Model:

The annual change in a variable is displayed as a percentage using growth rates. If a variable's growth rate is positive, it is said to be increasing over time; if it is negative, it is said to be decreasing over time. The model summary is displayed in the table below, along with the estimated standard error (0.069) and R-value (0.973). Figure 10 and Table 14 display the model growth.

Table 14. Shows the growth summary of the model District Hangu

R	**R Square**	**Adjusted R Square**	**Std. Error of the Estimate**
0.973	0.921	0.921	0.069
Population is the Independent Variable.			

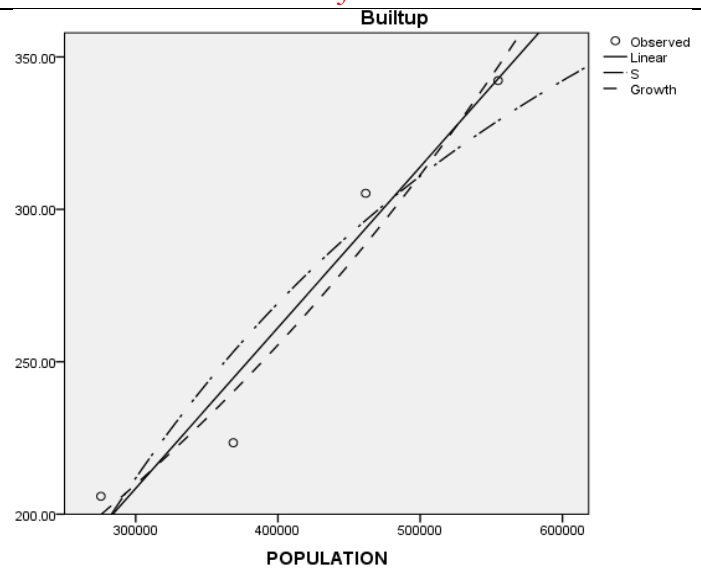

Figure 10. District Hangu, Built-up growth graph 2021-2050

Growth in Built-Up Area:

Built-up area 1991 and 2021: Results:

In 1991, the district Hangu built-up area was 111.88 km², and its population grew significantly. Due to the built-up area rapid population expansion in a single year, Figure 9 shows changes in the built-up area from 1991 to 2021. The maps below show the various changes in built-up area years (1991–2021).

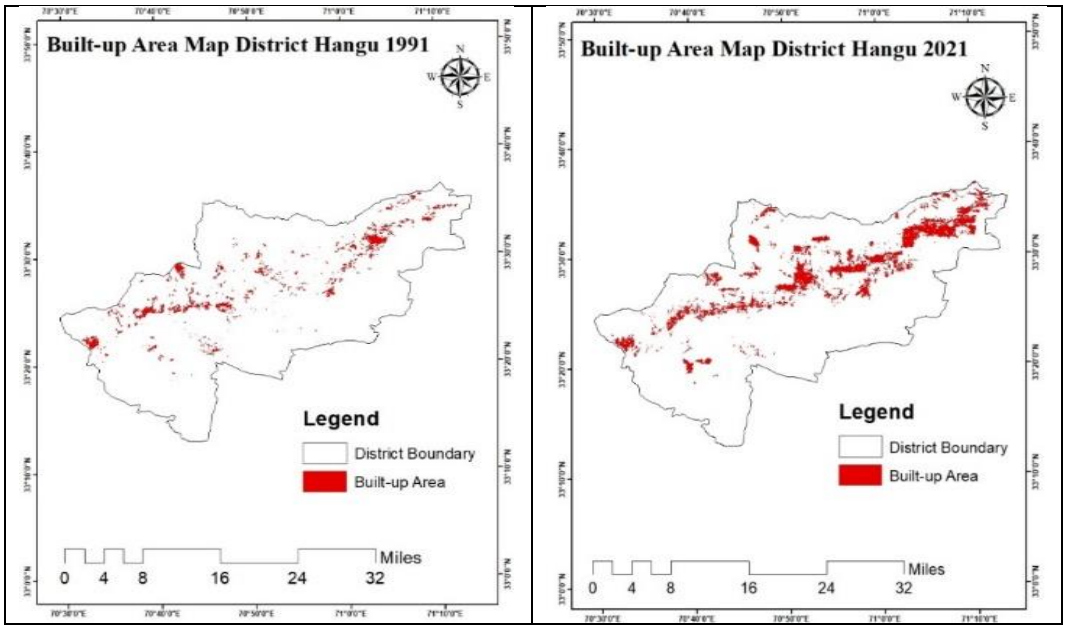

Figure 11. District Hangu, Built-up area from 1991-2021

The 2050 probability map for built-up land development in Hangu District suggests a 50–60% likelihood of urban expansion occurring along roads and near existing economic hubs. The map further indicates a 40% probability of built-up areas extending alongside roads. As expected, the likelihood of urban growth diminishes with increasing distance from both major and minor roads, as well as from established neighborhoods. Projections show that by 2050, the district's built-up area will grow from the current 149.24 km² by an additional 20 km², reaching a total of 161.22 km², reflecting the anticipated rate of expansion (Figure 12, table 15).

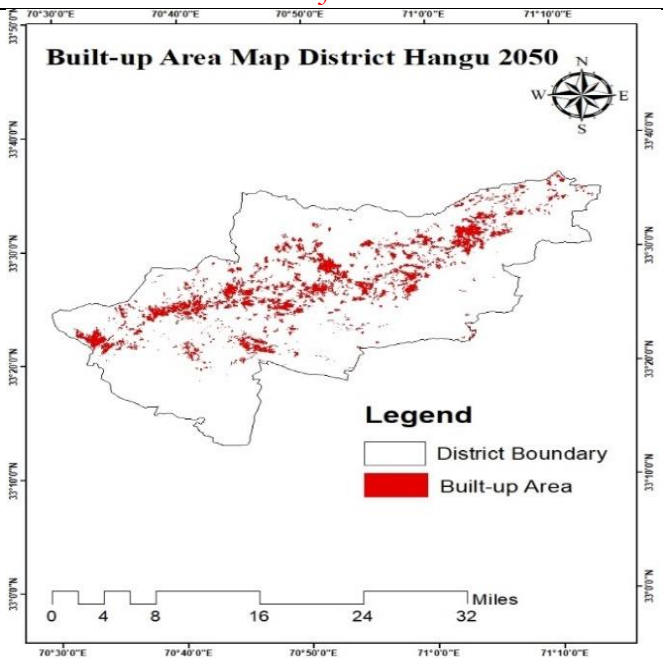

Figure 12. District Hangu, Built-up Area Map, 2050

Table 15. District Hangu, Population Growth and Built-up Area

Growth	Values
Population Growth (P 2050)	833,964
Population 2017	518,811
Bult-up area 2021	149.42 km^2
Built-up area 2050	161.22km^2

Discussions:

Land Use and Land Cover (LU/LC) analysis reveals significant changes in the landscape of Hangu District between 1991 and 2021, with the most prominent being the expansion of the built-up area from 111.88 km^2 to 149.24 km^2. This is a result of urbanization, population growth, and the increasing need for infrastructure and housing. Natural or underutilized land is frequently turned into residential and commercial areas as a result of such development. During the study period, vegetation covers also increased, from 577.58 km^2 to 622.32 km^2; however, the values varied in the years in between. This could indicate changes in agricultural practices, forestry initiatives, or the regrowth of natural vegetation. Consistent observation is necessary to determine whether this rise is sustainable, though.

From 42.60 km^2 to 49.42 km^2, the area under water bodies increased somewhat, most likely as a result of seasonal water retention, rainfall patterns, or small-scale water management. On the other hand, the amount of barren land dropped significantly, from 648.49 km^2 to 560.92 km^2. This decrease shows that once underutilized or degraded land has been put to good use, such as through farming, plantations, or urban development.

These LU/LC shifts demonstrate how human activity is changing the environment. Effective land use regulations and sustainable urban planning are necessary to control future expansion while maintaining ecological balance and natural resources in light of the steadily growing built-up regions.

The projected growth trends highlight notable demographic and spatial changes within the district. The population is expected to rise from 518,811 in 2017 to 833,964 by 2050, representing a significant increase that will inevitably intensify pressure on existing infrastructure, public services, and natural resources. In parallel, the built-up area is predicted to

expand from 149.42 km² in 2021 to 161.22 km² by 2050, reflecting a gradual yet steady pattern of urbanization. While the spatial expansion appears moderate compared to population growth, the imbalance between demographic increase and built-up area suggests potential challenges such as overcrowding, housing shortages, and strain on land resources. These findings emphasize the importance of implementing integrated urban planning strategies that can accommodate population growth while ensuring environmental sustainability and balanced land use.

Conclusion:

The current study evaluated and examined the reasons for the LU/LC shift in District Hangu over the four decades from 1990–2021. By utilizing remote sensing and GIS methodologies to analyze the LU/LC dynamics, four types of LU/LC have been identified. This study distinguished four LU/LC classes: barren land, water, vegetation, and built-up areas. The built-up area showed an increasing trend over four decades. Throughout the four study periods, the LU/LC change trend in the individual classes differed. The research indicated more barren land and less vegetation. A significant portion of the research areas consists of open, barren ground; this land use has also experienced the greatest LU/LC transition, progressively shifting into other classes. Providing households with food for sustenance has led to an expansion of vegetation land at the expense of current natural resources, but over time, this will shrink due to rapid population increase. According to the report, there is less vegetation in the research region because it increased from 43% to 45% of the study area between 1991 and 2021. A large proportion of the studied areas consists of open, barren ground; this land use has also experienced the greatest LU/LC transition, progressively shifting into other classifications. The data indicates a substantial increase in both population and built-up area over time. From 2017 to 2050, the population is projected to grow from 518,811 to 833,964, reflecting significant demographic expansion. Similarly, the built-up area is expected to rise from 149.42 km² in 2021 to 161.22 km² by 2050, indicating ongoing urban development. These trends suggest increased demand for infrastructure, housing, and resources in the coming decades, underscoring the need for sustainable urban planning and resource management.

References:

[1] M. S. A. Muhammad Arslan Ashraf, Iqbal Hussain, Rizwan Rasheed, Muhammad Iqbal, Muhammad Riaz, "Advances in microbe-assisted reclamation of heavy metal contaminated soils over the last decade: A review," *J. Environ. Manage.*, vol. 198, no. 1, pp. 132–143, 2017, doi: https://doi.org/10.1016/j.jenvman.2017.04.060.

[2] M. Brauer *et al.*, "Exposure assessment for estimation of the global burden of disease attributable to outdoor air pollution," *Environ. Sci. Technol.*, vol. 46, no. 2, pp. 652–660, Jan. 2012, doi: 10.1021/ES2025752/SUPPL_FILE/ES2025752_SI_005.ZIP.

[3] G. B. Chaolin Tan, Fei Weng Sui, Shang Chew, Youxiang, "Progress and perspectives in laser additive manufacturing of key aeroengine materials," *Int. J. Mach. Tools Manuf.*, vol. 170, p. 103804, 2021, doi: https://doi.org/10.1016/j.ijmachtools.2021.103804.

[4] S. Covaleda *et al.*, "Land-use effects on the distribution of soil organic carbon within particle-size fractions of volcanic soils in the Transmexican Volcanic Belt (Mexico)," *Soil Use Manag.*, vol. 27, no. 2, pp. 186–194, Jun. 2011, doi: 10.1111/J.1475-2743.2011.00341.X.

[5] D. R. F. Gerald R. Fowkes, "Comparison of global estimates of prevalence and risk factors for peripheral artery disease in 2000 and 2010: a systematic review and analysis," *Lancet*, vol. 382, no. 9901, pp. 1329–1340, 2013, [Online]. Available: https://www.thelancet.com/journals/lancet/article/PIIS0140-6736(13)61249-0/fulltext

[6] A. Geddes, "Half a Century of Population Trends in India: A Regional Study of Net Change and Variability, 1881-1931," *Geogr. J.*, vol. 98, no. 5/6, p. 228, Nov. 1941, doi:

10.2307/1787456.

[7] "World Population Data Sheet." Accessed: Jun. 08, 2024. [Online]. Available: https://www.prb.org/wp-content/uploads/2023/12/2023-World-Population-Data-Sheet-Booklet.pdf

[8] D. W. Huang *et al.*, "Extracting biological meaning from large gene lists with DAVID," *Curr. Protoc. Bioinforma.*, vol. Chapter 13, no. SUPPL. 27, 2009, doi: 10.1002/0471250953.BI1311S27,.

[9] A. Khan, S. Khan, M. A. Khan, Z. Qamar, and M. Waqas, "The uptake and bioaccumulation of heavy metals by food plants, their effects on plants nutrients, and associated health risk: a review," *Environ. Sci. Pollut. Res. 2015 2218*, vol. 22, no. 18, pp. 13772–13799, Jul. 2015, doi: 10.1007/S11356-015-4881-0.

[10] B. M. I. N. Abel Kadeba, "Land cover change and plants diversity in the Sahel: A case study from northern Burkina Faso," *Ann. For. Res.*, vol. 58, no. 1, 2015, [Online]. Available: https://www.afrjournal.org/index.php/afr/article/view/350

[11] J. M. E.F. Lambin, H.K. Gibbs, L. Ferreira, R. Grau, P. Mayaux, P. Meyfroidt, D.C. Morton, T.K. Rudel, I. Gasparri, "Estimating the world's potentially available cropland using a bottom-up approach," *Glob. Environ. Chang.*, vol. 23, no. 5, pp. 892–901, 2013, doi: https://doi.org/10.1016/j.gloenvcha.2013.05.005.

[12] X. H. Yanghao Li, Naiyan Wang, Jiaying Liu, "Demystifying Neural Style Transfer," *arXiv:1701.01036*, 2017, doi: https://doi.org/10.48550/arXiv.1701.01036.

[13] M. Livi-Bacci, "A Concise History of World Population," Feb. 2017, doi: 10.1002/9781119406822.

[14] M. S. Loudermilk, "Estimation of Fractional Dependent Variables in Dynamic Panel Data Models With an Application to Firm Dividend Policy," *J. Bus. Econ. Stat.*, vol. 25, no. 4, pp. 462–472, Oct. 2007, doi: 10.1198/073500107000000098.

[15] M. S. Abdoul Salam Ouedraogo, "High prevalence of extended-spectrum ß-lactamase producing enterobacteriaceae among clinical isolates in Burkina Faso," *BMC Infect. Dis.*, vol. 16, 2016, doi: 10.1186/s12879-016-1655-3.

[16] L. Roser, M., Ritchie, H., Ortiz-Ospina, E., & Rodés-Guirao, "World population growth," *Our world data*, 2013.

[17] Y. Samiullah, "Prediction of the Environmental Fate of Chemicals," *Book*, 1990, doi: 10.1007/978-94-009-2211-2.

[18] S. G. Setegn, R. Srinivasan, B. Dargahi, and A. M. Melesse, "Spatial delineation of soil erosion vulnerability in the Lake Tana Basin, Ethiopia," *Hydrol. Process.*, vol. 23, no. 26, pp. 3738–3750, Dec. 2009, doi: 10.1002/HYP.7476;JOURNAL:JOURNAL:10991085.

[19] M. Shafiq-Ul-hassan *et al.*, "Intrinsic dependencies of CT radiomic features on voxel size and number of gray levels," *Med. Phys.*, vol. 44, no. 3, pp. 1050–1062, Mar. 2017, doi: 10.1002/MP.12123;WEBSITE:WEBSITE:AAPM;PAGE:STRING:ARTICLE/CHAPTER.

[20] M. Shirazi, R. Zane, and D. Maksimovic, "An autotuning digital controller for DC-DC power converters based on online frequency-response measurement," *IEEE Trans. Power Electron.*, vol. 24, no. 11, pp. 2578–2588, 2009, doi: 10.1109/TPEL.2009.2029691.

[21] Arch G. Woodside, "Moving beyond multiple regression analysis to algorithms: Calling for adoption of a paradigm shift from symmetric to asymmetric thinking in data analysis and crafting theory," *J. Bus. Res.*, vol. 66, no. 4, pp. 463–472, 2013, doi: https://doi.org/10.1016/j.jbusres.2012.12.021.

[22] C. Wrigley and K. Straker, "Designing innovative business models with a framework that promotes experimentation," *Strateg. Leadersh.*, vol. 44, no. 1, pp. 11–19, Jan. 2016, doi: 10.1108/SL-06-2015-0048/FULL/XML.

[23] X.-P. Z. Xiao-Lin Xie, Yiu-Wing Mai, "Dispersion and alignment of carbon nanotubes in polymer matrix: A review," *Mater. Sci. Eng. R Reports*, vol. 49, no. 4, pp. 89–112, 2005, doi: https://doi.org/10.1016/j.mser.2005.04.002.

[24] X. Z. Chaodong Tan, Song Wang, Hanwen Deng, Guoqing Han, Guanghao Du, Wenrong Song, "The Health Index Prediction Model and Application of PCP in CBM Wells Based on Deep Learning," *Geofluids*, 2021, doi: https://doi.org/10.1155/2021/6641395.

[25] E. G. Stein Emil Vollset, "Fertility, mortality, migration, and population scenarios for 195 countries and territories from 2017 to 2100: a forecasting analysis for the Global Burden of Disease Study," *Lancet*, vol. 396, no. 10258, pp. 1285–1306, 2020, doi: 10.1016/S0140-6736(20)30677-2.

[26] L. F. The MINERvA collaboration, "Measurement of Muon Antineutrino Quasi-Elastic Scattering on a Hydrocarbon Target at E_ν ~ 3.5 GeV," *Phys. Rev. Lett.*, 2024, doi: https://doi.org/10.1103/PhysRevLett.111.022501.